CMS Physics Analysis Summary

Contact: cms-pag-conveners-susy@cern.ch 2013/09/07

Search for SUSY Partners of Top and Higgs Using Diphoton Higgs Decays

The CMS Collaboration

Abstract

We present results of a search for a "natural" SUSY scenario with gauge-mediated breaking. We select events in which there are two photons comprising a Higgs boson candidate, at least two b-jets and missing transverse energy. Using 19.5 fb^{-1} of proton-proton collisions at $\sqrt{s}$ = 8 TeV, recorded in the Compact Muon Solenoid experiment we find no evidence of a signal and set lower limits at the 95% confidence level on the stop mass below 360 to 410 GeV, depending on the higgsino mass.

1 Introduction

The recent measurements of the properties of the new boson by ATLAS [1, 2] and CMS [3, 4] confirm that it is likely a standard model (SM) Higgs boson. One of the most important problems in particle physics, now that the Higgs boson is established, is to understand why its mass is so small compared to the Planck Scale. Supersymmetry (SUSY) has long offered an elegant solution to this hierarchy problem. Although experimental searches have found no signs of it so far, and the simplest SUSY models become increasingly more constrained, there remain very large yet unprobed areas in SUSY parameter space that would still be "natural", i.e. have a fairly small amount of fine tuning.

The essential requirement of "natural" SUSY is that the masses of the super-partners of the top quark and the Higgs boson, the stop and the higgsino, are light (see, for example, [5, 6]). In this note we describe a search for events with a topology motivated by SUSY with a Gauge-Mediated SUSY Breaking (GMSB) model [7–10]. We assume a "minimal" number of light SUSY partners, namely right-handed stops and higgsinos. The latter are the lightest chargino ($\widetilde{\chi}_1^+$) and neutralinos ($\widetilde{\chi}_1^0, \widetilde{\chi}_2^0$) and are almost mass-degenerate.

Pairs of higgsinos are produced either directly through electroweak production or through right-handed stop–anti-stop pairs (strong production) with cascade decays

$$\widetilde{t}_R \to b\widetilde{\chi}_1^+ \text{ or } t\widetilde{\chi}_i^0, \tag{1}$$

where $i = 1, 2$. The $\widetilde{\chi}_1^+$ ($\widetilde{\chi}_2^0$) subsequently decays into a very off-shell W (Z) boson and a $\widetilde{\chi}_1^0$. The near mass degeneracy requires the off-shell W (Z) boson decay products to be very soft.

The final decay of the neutralino in all cascades is

$$\widetilde{\chi}_1^0 \to H\widetilde{G} \text{ or } Z\widetilde{G}, \tag{2}$$

where $\widetilde{G}$ is the gravitino. The branching fractions of $\widetilde{\chi}_1^0$ depend on SUSY parameters. For a significant portion of the parameter space, for example for low values of $\tan\beta$, the ratio of the up-type to down-type Higgs vacuum expectation values, and negative values of the supersymmetric Higgs mass term μ, Higgs bosons dominate the neutralino decays [11].

The final state we are interested in, therefore, has two b-jets, two Higgs bosons, and some missing transverse energy from the gravitinos, as shown in Figure 1. In order to suppress SM backgrounds, i.e. from top quark pair production, we take advantage of the known Higgs boson mass and require at least one of the Higgs bosons to decay into two photons. This approach also allows us to use the diphoton mass sidebands for a robust and data driven estimate of the background, which is dominated by QCD production of $\gamma\gamma b\bar{b}$ events and $\gamma b\bar{b} + j$ events in which the jet is misidentified as a photon.

2 Data and Simulation

We use the 19.5 fb^{-1} of data collected during the LHC 8 TeV running with the CMS detector, which is described in detail elsewhere [12]. Events are required to pass a suite of diphoton triggers requiring two photon candidates, passing mild shower shape and isolation requirements, with transverse energies above 36 and 22 GeV for the leading and the trailing photon respectively.

We simulate the signal events for a grid of higgsino and stop masses using MADGRAPH 5 v.1.5.4 [13] and PYTHIA 6.4 [14] generators and fast GEANT simulation of the CMS detector [15].

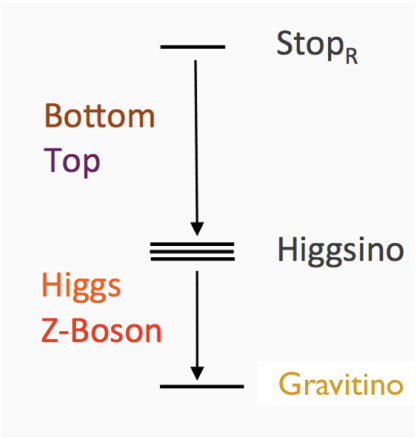

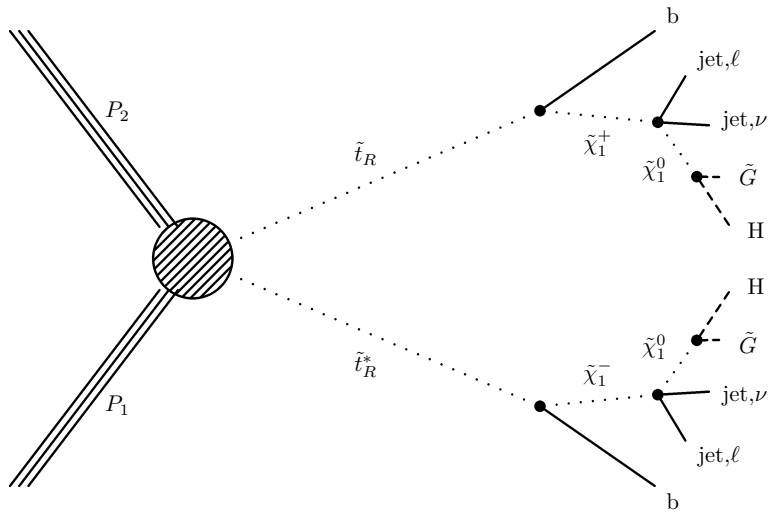

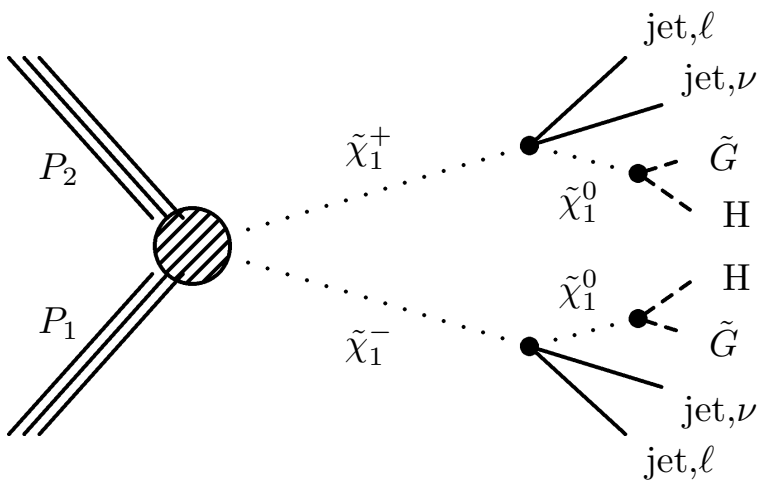

Figure 1: *Top:* The spectrum of the minimal model we consider. *Center:* Example Feynman diagram of strong production. *Bottom:* Example Feynman diagram of electroweak production. The jets or leptons resulting from transitions between higgsinos are extremely soft in both diagrams due to the near mass degeneracy of the chargino and the neutralino.

The next-to-leading order (NLO) cross sections (see Figure 2) are calculated using PROSPINO [16–21]. We set the higgsino mass splittings to 5 GeV, and use 100% branching fraction for $\widetilde{\chi}_1^0 \to H\widetilde{G}$ decay.

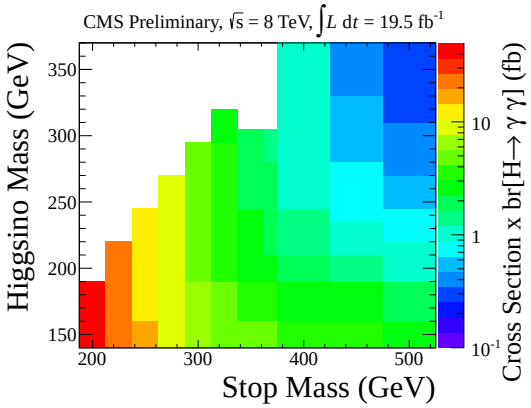

Figure 2: Cross section x $Br[H \to \gamma\gamma]$ for the generated MC points.

3 Object Reconstruction and Identification

Photon candidates are reconstructed from the energy deposits in the electromagnetic calorimeter, grouping its channels into superclusters [22]. We require photons to register in the barrel portion of the calorimeter ($|\eta| < 1.4442$, where $\eta = -\ln[\tan(\theta/2)]$ and θ is the polar angle of the particle with respect to the counterclockwise proton beam direction) and pass shower shape and isolation requirements. To reject electrons misidentified as photons, we also require that photons do not have associated hit patterns in the pixel detector consistent with a track. Photon energies are calculated using multivariate regression following the method described in reference [23].

We use the particle flow (PF) algorithm [24] to reconstruct individual particles (PF candidates) in the events, combining all available sub-detector information in a coherent and optimal manner. Jets are reconstructed from the PF particles using the anti-k_T [25] algorithm. The two leading identified photons are removed from the jet list using a ΔR cut of 0.6 and a $\Delta\phi$ cut of 0.05 radians (where $\Delta\phi$ is the difference in azimuthal angles of the photon and the jet, and where $\Delta R = \sqrt{(\Delta\phi)^2 + (\Delta\eta)^2}$). We apply transverse momentum (p_T) and η dependent corrections to the jet energies to account for residual effects of non-uniform detector response. The pileup contribution is estimated and subtracted from the jet energy using the jet area method [26] on an event-by-event basis. The combined secondary vertex (CSV) algorithm [27] is employed to identify jets that come from a b-quark.

The missing transverse energy ($E_{\mathrm{T}}^{\mathrm{miss}}$) in the event is computed as minus the vectorial sum of the transverse momenta of all PF candidates [24]. We also calculate the following event kinematics variables:

- H_{T}: the scalar sum of the p_T of all the jets in the event,
- B_T: the scalar sum of the p_T of all the CSV-LOOSE b-jets in the event,
- S_T: the scalar sum of the $E_{\mathrm{T}}^{\mathrm{miss}}$, the H_{T}, and the p_T of photon candidates,
- H_{T}^{miss}: the vectoral sum of the p_T of all the jets in the event.

4 Event Selection and Categorization

The events are selected if they have at least two identified photons, with transverse energies above 40 and 25 GeV for the leading and trailing photons respectively. Events are also required to have at least two jets with transverse energy above 30 GeV and $|\eta| < 2.4$ and satisfying the CSV-LOOSE requirements, and at least one of which also must pass the CSV-MEDIUM requirement.

The events with diphoton mass between 120 and 131 GeV constitute the *signal sample*, while the events with mass between 103 and 118 GeV and between 133 and 163 GeV comprise the *lower sideband* and *upper sideband* samples respectively.

The SUSY signature we look for has multiple b-jets. The dominant decay of the Higgs boson is to b-quarks, and, in case of strong production, one expects two more b-jets from the stop to higgsino decay. We exploit this by separating events into three categories as follows:

1. events with at least one additional CSV-LOOSE b-jet in addition to the two (i.e. events with three or more b-jets)
2. events for which the invariant mass of the two b-jets is within a Higgs mass window, from 95 to 155 GeV
3. all other events.

The distribution of signal events between the three categories depends on the stop and higgsino masses. For small mass differences between the stop and the higgsino, most of the signal populates category 2, while for large mass differences categories 1 and 3 dominate.

The search is performed independently in the three categories and the results are combined, leading to up to a 35% improvement in expected SUSY cross-section limits compared to the analysis without categorization.

5 Background Prediction

The background from standard model Higgs production was found to be negligible for this analysis in Monte Carlo simulations. We use sidebands around the Higgs mass in the diphoton mass distribution to derive a robust data driven measure of all non-Higgs standard model background processes. The background predictions are shown in Figures 3 and 4 as the red hatched rectangles.

The background is dominated by QCD production of $\gamma\gamma b\bar{b}$ events and $\gamma b\bar{b} + j$ events in which a jet is misidentified as a photon. We measured the component of the background due to electrons misidentified as photons in data and found that this is a minute contribution. In any case, the sideband method allows us to accurately determine the standard model background regardless of its composition.

We divide the diphoton mass distribution into three regions: a narrow signal region on the Higgs mass and two sidebands on either side of it, with 2 GeV buffer regions in between. We fit the diphoton distribution using a power law from 105 to 160 GeV. The region from 118 to 133 GeV, corresponding to the signal region plus the buffers, is excluded from the fitter's consideration to prevent potential signal from affecting the background estimate. The result

of the fit is used to calculate the normalization of the background. We explored the effects of various other fit functions and resulting variations in the estimated background yields are well described by the uncertainty in the fit function integral from the power law fit.

We then obtain distributions of our kinematic variables of interest for both the upper and lower sidebands. This provides us with two independent estimates for the distributions of the standard model background. In determining the uncertainty in each of these estimates we take into account the statistical correlation between the content of each bin and the entire sideband.

We do not observe significant correlations between the diphoton mass and other kinematic variables. However, to account for possible correlations, we conservatively assume that the background yield is bounded by independent estimates from the upper and lower sidebands, and calculate the background prediction and its error as follows. We form our main background estimate by taking the bin-by-bin average of the two background estimates from the sidebands. We take half the difference, bin-by-bin, between the two estimates as a systematic uncertainty so that the uncertainty in the main background estimate spans the difference between the two estimates. For $E_{\mathrm{T}}^{\mathrm{miss}}$ the uncertainty is statistics limited and the systematic uncertainty is relatively unimportant.

6 Results

The observed distributions of $E_{\mathrm{T}}^{\mathrm{miss}}$ are shown in Figure 3 separately for the three event categories, and for the entire dataset, together with the data-driven background expectation and the expected distributions for three signal mass points. Figure 4 shows the distributions of H_{T}, S_T, B_T, and H_{T}^{miss} for the data, the background predictions, and representative signal mass points. These four variables and $E_{\mathrm{T}}^{\mathrm{miss}}$ have somewhat complementary sensitivity, as can be seen in the relative differences between the distributions of predicted background and that of signal for the three mass points.

Table 1 shows the total event counts, the total background predictions, and expected signal yields, for the three event categories. The background estimates for each category are from the power-law fits to the diphoton mass ($M_{\gamma\gamma}$) distributions in the corresponding category. The uncertainties on the background estimates here are due entirely to uncertainties in the integrals of the fit functions. The observations are in agreement with the background predictions.

Table 1: Expected and observed event counts. The yields for three signal points are shown for comparison indicating M_{stop} and $M_{higgsino}$ respectively.

	On H mass	Off H mass	$3+$ b-jets
signal 350 / 135 GeV	2.0	6.8	10.7
signal 300 / 290 GeV	10.1	3.9	2.1
signal 400 / 300 GeV	1.4	2.8	4.0
expected background	10.8 ± 2.1	28.7 ± 3.0	6.3 ± 1.5
observed	7	33	6

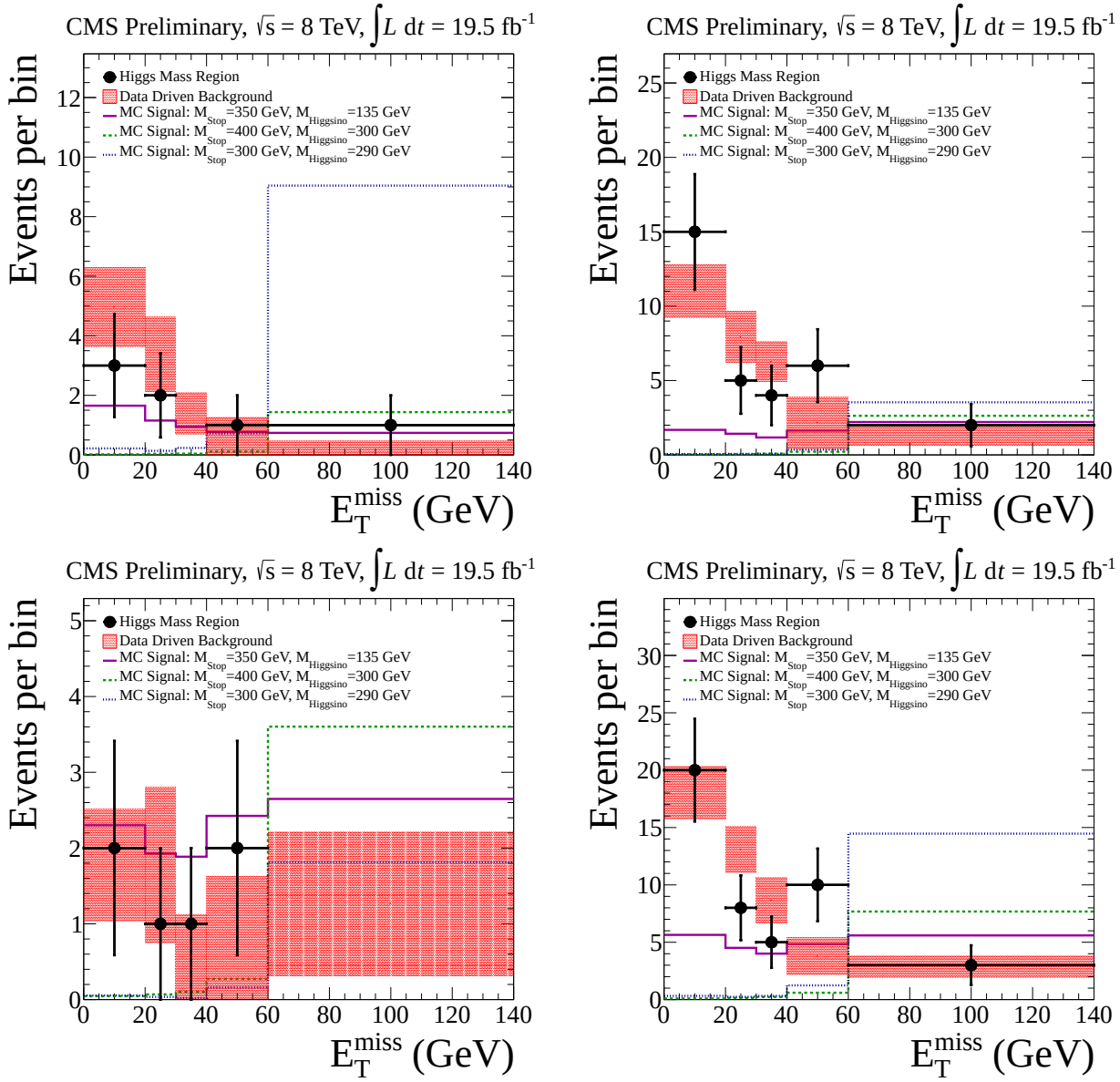

Figure 3: $E_{\mathrm{T}}^{\mathrm{miss}}$ distributions for the data, background predictions, and representative signals for the three b-jet categories (see Section 4). Upper left: the 2 b-jets category with M_{bb} on the Higgs mass. Upper Right: the 2 b-jets category with M_{bb} off the Higgs mass. Lower left: the 3 or more b-jets category. Lower right: the sum of the three categories. Signal point masses are in units of GeV. For each histogram, the last bin includes the overflow. The first three plots hold all the data and background estimates used for limit setting.

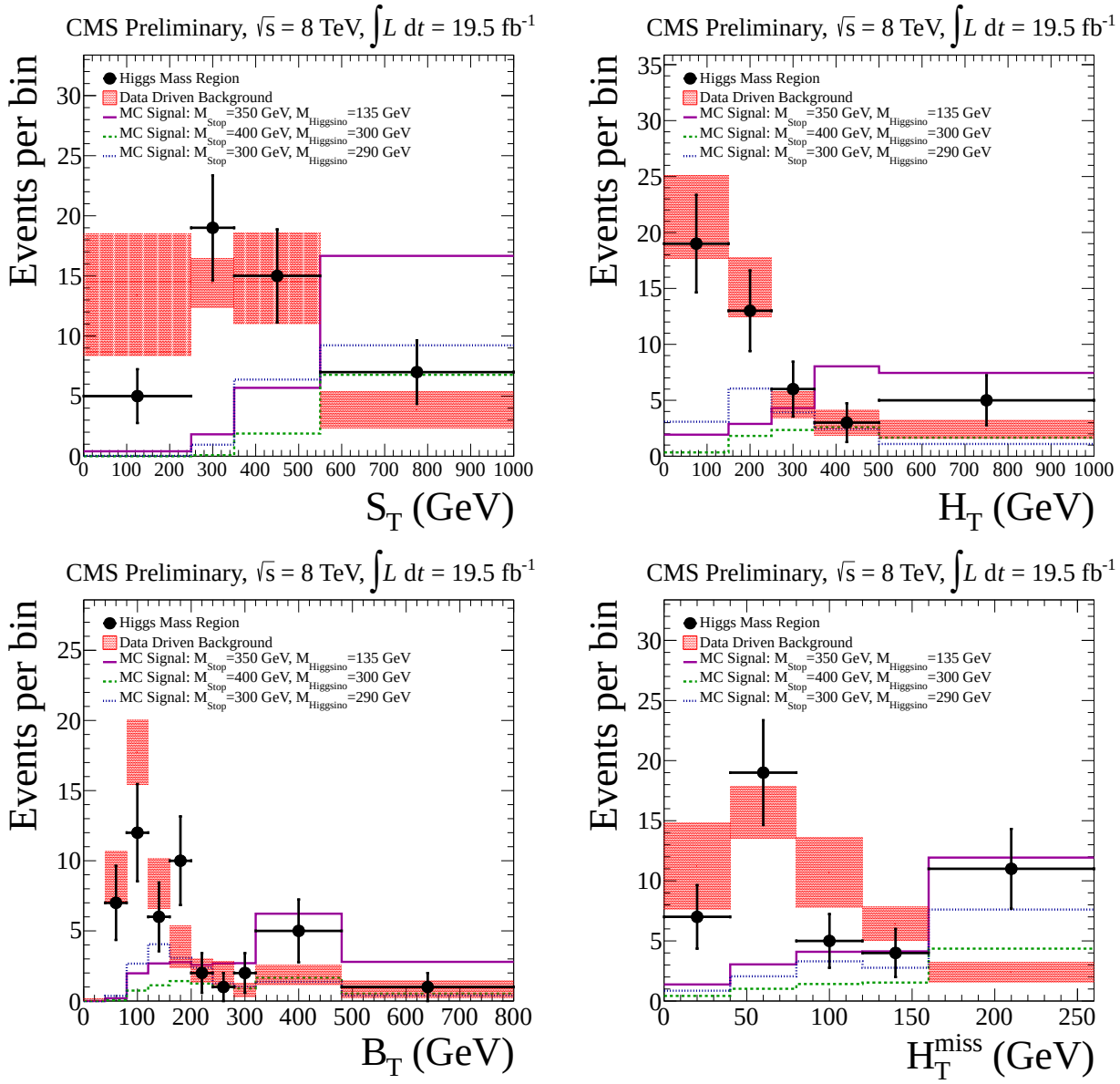

Figure 4: The distributions of H_{T}, S_T, B_T and H_{T}^{miss} for the data, background predictions (shaded rectangles), and selected Monte Carlo mass points (color lines). For each histogram, the last bin includes the overflow.

7 Statistical Interpretation

Since the data agree with the expected background we proceed to set limits on the SUSY model described above. We calculate the expected limits using a variety of kinematic variables and determined that $E_{\mathrm{T}}^{\mathrm{miss}}$ is the single most sensitive variable. The observe $E_{\mathrm{T}}^{\mathrm{miss}}$ distributions for the three b-jet categories, shown in Figure 3, together with the signal and background expectations listed in Table 1, are used as input to the limit-setting.

We use a frequentist LHC-style profiled likelihood test statistics [28–30]. For each model mass point, the modified frequentist CL_S criterion is used to calculate upper limits on the cross section for the model.

The dominant uncertainty in the analysis is the statistical uncertainty of the background prediction. The sources of systematics on the signal include the uncertainties in integrated luminosity [31], the diphoton trigger efficiency, the photon reconstruction and identification efficiency, the photon resolution uncertainty, the jet energy scale, and the b-jet identification efficiency. All systematic uncertainties are correlated between the b-jet categories and are treated as nuisance parameters in the likelihood, profiled according to their estimated value (see Table 2).

Figure 5 shows the limits we obtain for the GMSB model in the stop-higgsino mass plane. Depending on the higgsino mass, and conservatively using minus-one-standard-deviation value for the theoretical cross section, we are able to exclude stop masses below 360 to 410 GeV with 95% confidence, corresponding to the region to the left of the thick black line in Figure 5.

Table 2: Sources of systematic uncertainties on signal.

Source of Uncertainty	Value
Trigger efficiency uncertainty	0.1%
Photon efficiency uncertainty	1%
Photon resolution uncertainty	1%
B-jet identification uncertainty	shape uncertainty: 1-5% for 2 B-jets, 6-17% for 3 B-jets
Jet energy scale uncertainty	shape uncertainty 7-43% for $20 < E_{\mathrm{T}}^{\mathrm{miss}} < 40$ GeV; negligible elsewhere
Luminosity uncertainty	4.4%
Signal theoretical cross-section uncertainty	$\sim$15% [32]

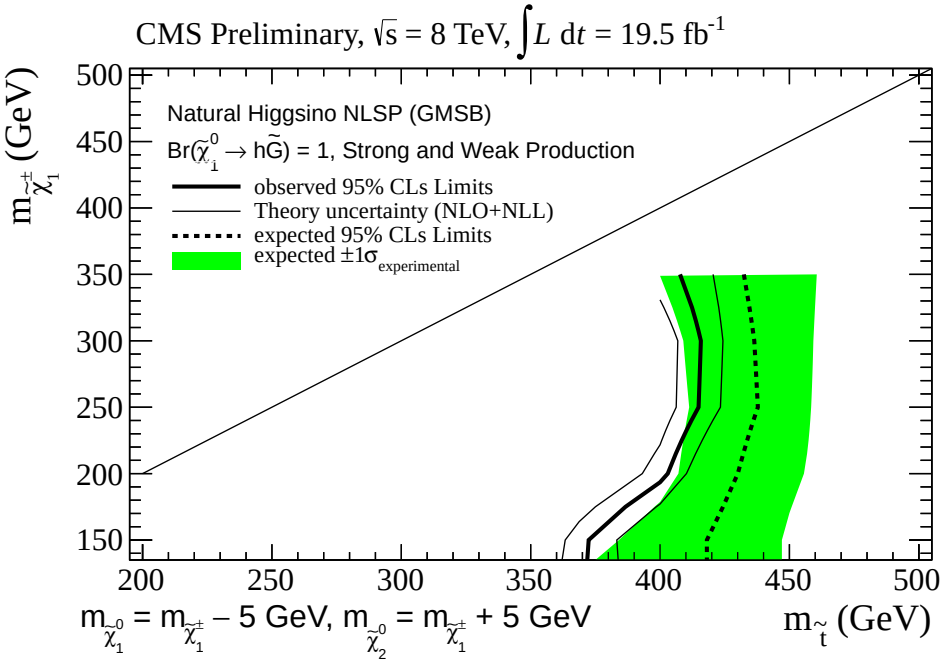

Figure 5: Limit on stop and higgsino masses using *b*-jet categories. The regions to the left of the contours are expected (dashed black) and observed (bold black) to be excluded with 95% confidence.

8 Conclusion

We have performed a search for a "natural" SUSY scenario with light higgsinos and a stop using Higgs tagging in the diphoton decay mode in a final state containing at least two photons, two or more *b*-jets, and missing transverse energy. No evidence for a signal is observed, and 95% CL limits are set in the stop - higgsino mass plane, excluding a significant portion of the "natural" parameter space up to stop masses of 410 GeV.

References

[1] "Study of the spin of the new boson with up to 25 fb^{-1} of ATLAS data", ATLAS Conference Note ATLAS-CONF-2013-040, CERN, Geneva, (Apr, 2013).

[2] "Combined coupling measurements of the Higgs-like boson with the ATLAS detector using up to 25 fb^{-1} of proton-proton collision data", ATLAS Conference Note ATLAS-CONF-2013-034, CERN, Geneva, (Mar, 2013).

[3] CMS Collaboration, "Study of the Mass and Spin-Parity of the Higgs Boson Candidate Via Its Decays to Z Boson Pairs", *Phys.Rev.Lett.* **110** (2013) 081803, doi:10.1103/PhysRevLett.110.081803, arXiv:1212.6639.

[4] "Properties of the observed Higgs-like resonance using the diphoton channel", CMS Physics Analysis Summary CMS-PAS-HIG-13-016, CERN, Geneva, (2013).

[5] R. Barbieri and G. Giudice, "Upper Bounds on Supersymmetric Particle Masses", *Nucl.Phys.* **B306** (1988) 63, doi:10.1016/0550-3213(88)90171-X.

[6] M. Papucci, J. T. Ruderman, and A. Weiler, "Natural SUSY Endures", *JHEP* **1209** (2012) 035, doi:10.1007/JHEP09(2012)035, arXiv:1110.6926.

[7] S. Dimopoulos, M. Dine, S. Raby, and S. D. Thomas, "Experimental signatures of low-energy gauge mediated supersymmetry breaking", *Phys.Rev.Lett.* **76** (1996) 3494–3497, doi:10.1103/PhysRevLett.76.3494, arXiv:hep-ph/9601367.

[8] S. Ambrosanio et al., "Search for supersymmetry with a light gravitino at the Fermilab Tevatron and CERN LEP colliders", *Phys.Rev.* **D54** (1996) 5395–5411, doi:10.1103/PhysRevD.54.5395, arXiv:hep-ph/9605398.

[9] K. T. Matchev and S. D. Thomas, "Higgs and Z boson signatures of supersymmetry", *Phys.Rev.* **D62** (2000) 077702, doi:10.1103/PhysRevD.62.077702, arXiv:hep-ph/9908482.

[10] K. Howe and P. Saraswat, "Excess Higgs Production in Neutralino Decays", *JHEP* **1210** (2012) 065, doi:10.1007/JHEP10(2012)065, arXiv:1208.1542.

[11] P. Meade, M. Reece, and D. Shih, "Prompt Decays of General Neutralino NLSPs at the Tevatron", *JHEP* **1005** (2010) 105, doi:10.1007/JHEP05(2010)105, arXiv:0911.4130.

[12] CMS Collaboration, "The CMS experiment at the CERN LHC", *JINST* **3** (2008) S08004, doi:10.1088/1748-0221/3/08/S08004.

[13] J. Alwall et al., "MadGraph 5 : Going Beyond", *JHEP* **1106** (2011) 128, doi:10.1007/JHEP06(2011)128, arXiv:1106.0522.

[14] T. Sjöstrand, S. Mrenna, and P. Z. Skands, "PYTHIA 6.4 Physics and Manual", *JHEP* **0605** (2006) 026, doi:10.1088/1126-6708/2006/05/026, arXiv:hep-ph/0603175.

[15] CMS Collaboration, "The fast simulation of the CMS Detector at the LHC", in *International Conference on Computing in High Energy and Nuclear Physics (CHEP 2010). J. Phys.: Conference Series* 331 (2011) 032049. doi:10.1088/1742-6596/331/3/032049.

[16] M. Kramer et al., "Supersymmetry production cross sections in pp collisions at $\sqrt{s} = 7$ TeV", arXiv:1206.2892.

[17] W. Beenakker, R. Hopker, M. Spira, and P. Zerwas, "Squark and gluino production at hadron colliders", *Nucl.Phys.* **B492** (1997) 51–103, doi:10.1016/S0550-3213(97)80027-2, arXiv:hep-ph/9610490.

[18] A. Kulesza and L. Motyka, "Threshold resummation for squark-antisquark and gluino-pair production at the LHC", *Phys.Rev.Lett.* **102** (2009) 111802, doi:10.1103/PhysRevLett.102.111802, arXiv:0807.2405.

[19] W. Beenakker et al., "Soft-gluon resummation for squark and gluino hadroproduction", *JHEP* **0912** (2009) 041, doi:10.1088/1126-6708/2009/12/041, arXiv:0909.4418.

[20] W. Beenakker et al., "Squark and Gluino Hadroproduction", *Int.J.Mod.Phys.* **A26** (2011) 2637–2664, doi:10.1142/S0217751X11053560, arXiv:1105.1110.

[21] W. Beenakker, R. Hopker, and M. Spira, "PROSPINO: A Program for the production of supersymmetric particles in next-to-leading order QCD", arXiv:hep-ph/9611232.

[22] "Photon reconstruction and identification at sqrt(s) = 7 TeV", CMS Physics Analysis Summary CMS-PAS-EGM-10-005, CERN, 2010. Geneva, (2010).

[23] "Updated measurements of the Higgs boson at 125 GeV in the two photon decay channel", CMS Physics Analysis Summary CMS-PAS-HIG-13-001, CERN, Geneva, (2013).

[24] CMS Collaboration, "Commissioning of the Particle-Flow Reconstruction in Minimum-Bias and Jet Events from pp Collisions at 7 TeV", *CMS PAS* **PFT-10-002** (2010).

[25] M. Cacciari, G. P. Salam, and G. Soyez, "The anti-k_t jet clustering algorithm", *JHEP* **04** (2008) 063, doi:10.1088/1126-6708/2008/04/063, arXiv:0802.1189.

[26] M. Cacciari and G. P. Salam, "Pileup subtraction using jet areas", *Physics Letters B* **659** (2008), no. 12, 119 – 126, doi:http://dx.doi.org/10.1016/j.physletb.2007.09.077.

[27] CMS Collaboration, "b-Jet Identification in the CMS Experiment", *CMS PAS* **BTV-11-004** (2011).

[28] ATLAS and CMS Collaborations, LHC Higgs Combination Group, "Procedure for the LHC Higgs boson search combination in Summer 2011", ATL-PHYS-PUB/CMS NOTE 2011-11, 2011/005, (2011).

[29] T. Junk, "Confidence level computation for combining searches with small statistics", *Nucl. Instrum. Meth. A* **434** (1999) 435, doi:10.1016/S0168-9002(99)00498-2, arXiv:hep-ex/9902006.

[30] A. L. Read, "Presentation of search results: The CL(s) technique", *J. Phys. G* **28** (2002) 2693, doi:10.1088/0954-3899/28/10/313.

[31] CMS Collaboration, "CMS Luminosity Based on Pixel Cluster Counting - Summer 2012 Update", CMS Physics Analysis Summary CMS-PAS-LUM-12-001, CERN, Geneva, (2012).

[32] M. Kramer et al., "Supersymmetry production cross sections in pp collisions at $\sqrt{s} = 7$ TeV", arXiv:1206.2892.